NEURAL NETWORK AND WAVELETS MODEL IN SEISMIC LOCATION FOR THE CENTRAL ANDES OF BOLIVIA

Estela Minaya, Percy Aliaga, Guido Avila, Cristina Condori, and Alejandro Córdova

Observatorio San Calixto

Sponsored by Army Space Defense and Missile Command

Contract No. F49620-97-1-0214

ABSTRACT

The location of seismic events in the Central Andes of Bolivia frequently displays differences between the reports by international agencies such as the International Data Center (IDC) or the Preliminary Determination of Epicenters (PDE) and those obtained from the National network. Also observed is an instability for different algorithms of location. The main cause of this instability is the dispersed azimuth distribution and the small number of seismic stations that are used to locate the events. Other factors that can cause this instability are marked attenuation of the S phase in earthquakes located in the south zone of Bolivia, or phases recorded as a consequence of the complex crustal structure that includes several refracting layers causing abrupt changes of period and amplitude.

In our first stage of investigation, we proposed to develop an artificial and automatic method that accomplishes localization using a Neural Network on Radial Bases Functions (NNRBF) by applying a Gaussian function to the coda of the seismic signal and its location parameters. Our results show that the NNRBF requires a better approximation of the training parameters with the activating functions.

In our second stage of investigation, we used a wavelet method instead of a Gaussian function to try to retain the maximum information recorded in the seismic signal when we applied the filters. This procedure applies the discrete wavelet transform to decompose the seismic noise, based on the Haar wavelet (or first Debauchies decomposition) with an alternating introduction in the NNRBF algorithm. Initially this methodology was tested with earthquakes in the central zone of Bolivia where the occurrence of seismic events is frequent and waveforms are less complex than in the rest of the region.

The 23 earthquakes tested that occurred in 2000 and consisting of magnitudes (Ml) greater than 3 were analyzed with a success rate of 83%. This first result leads us to consider using this technique as a solution for the problem involving a small number of stations and the dispersed azimuth distribution, thus increasing the database of seismic events and identifying mislocated events as 17% of the data analyzed. We will continue our investigations to determine the limitations of this method by testing it in the remaining zones of Bolivia.

OBJECTIVE

The objective of this research was to find a model (or method) for automatic localization that allows improvement in the localization of seismic events occurring in zones of complex crust structure, with few seismic stations and a disperse azimuthal distribution across them. The model would use Artificial Intelligence (AI) based on a Neuronal Networks on Radial Bases Functions (NNRBF) and the Wavelets method for treatment of seismic signals.

RESEARCH ACCOMPLISHED

One of the most concrete problems of localization precision has been the 1998 earthquake that occurred in the central region of Bolivia. Differences in localization, (Avila, 2000), reported by international agencies (IDC, PDE, ISC) and those obtained from the Bolivian National Network are clear and stated below on both Table 1 and Figure 1.

Table 1. Locations for the earthquake occurred on May 22, 1998 in the central region of Bolivia.

Source	Time	Latitude	Longitude	Depth
IDC	04 48 48.2	17.54	65.14	34
PDE o NEIC	04 48 50.4	17.73	65.43	24
ISC	04 41 50.5	17.85	65.53	24
Harvard CMT	04 49 02.5	17.60	65.20	15
3DGRIDLOC	04 48 46.2	17.81	65.10	1
3DGRIDLOC, 5km	04 48 45.2	17.92	65.18	1
OSC, French	04 48 44.8	17.88	65.05	9
OSC, Lienert	04 48 43.6	17.80	65.057	13
Isoseismals		17.85	65.16	11

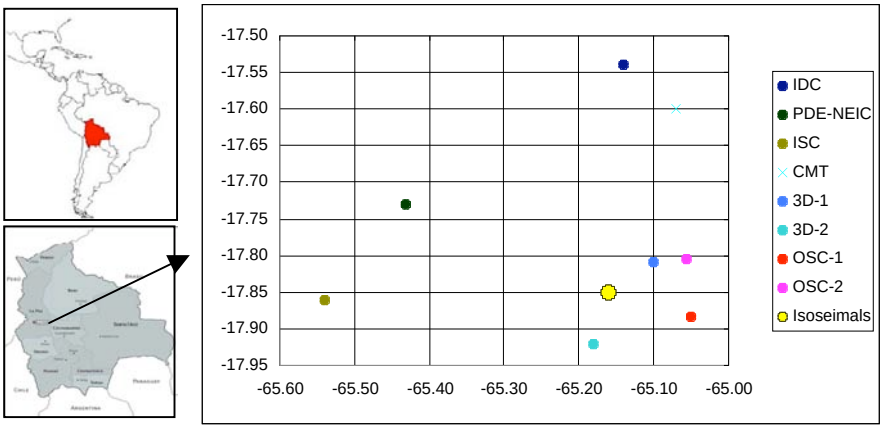

Figure 1. Map showing the locations of Table 1.

As the earthquake of May 22, 1998, there are many other events with the same problem, and the necessity for an automatic seismic localization model became imperious and was mainly based on the following premise: “A model is the explicit interpretation of what is understood from a situation or the idea about that situation. It may be expressed in mathematical or symbolic terms, or in words; but in essence it is a description of entities, processes, attributes and the relationship between them”, Pressman (1993).

METHODOLOGY

The seismic location model, proposed by Aliaga (2002), is composed of the elements shown in Figure 2. The task of the neuronal network was to classify a signal from an existing signal. It asks for signals previously localized with standard methods to be stored for training and searching. In order to obtain the results, an approximation of the maximum and minimum variations between training signals and the entry signal (or signal to be located) is used, and is determined by the Mean Squared Error (MSE or bias). The epicenters of the training signal (obtained by standard or traditional methods) are considered as provisional or previous localization for the entry signal. Once the neural network selection is concluded, the event is located using the Geiger method.

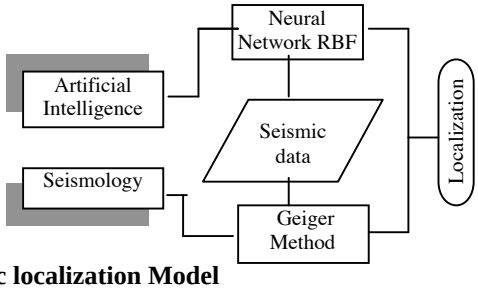

Figure 2. Components of the seismic localization Model

The following example shows this process. There is an entry signal of a seismic event that will be classified in relation to the training signals A and B. The entry signal is similar to the training signal A shown in Figure 3. Consequently the provisional epicenter of the entry signal is training signal A. However we fully acknowledge that there will always be a variation between the entry signal and the result because of the fact that no two seismic signals are identical.

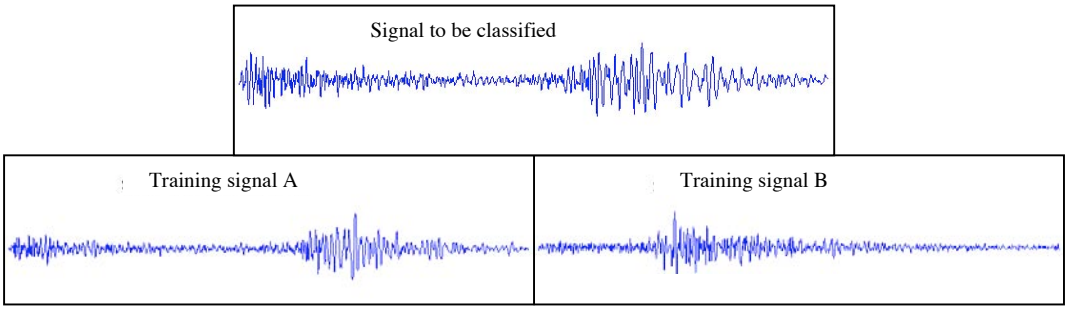

Figure 3. Example of an entry signal to be classification with the NNFRB.

In the final stage, seismic localization is obtained with the Geiger method, which employs localization parameters obtained in the neuronal network process as its requirement.

Theoretical analysis

The Neural Network on Radial Bases Functions is built with activation functions. In the beginning, several models were employed (linear or non-linear) as well as several network groups (for a single layer or multi layer). However the Neural Network on Radial Bases Functions (NNRBF) has been traditionally associated to a single layer network (Figure 4).

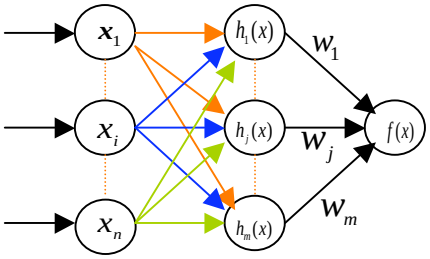

$$MSE = s = \sum_{i=1}^{p} (y_i - f(x_i))^2 \qquad \text{[Equation 1]}$$

$$f(x) = \sum_{j=1}^{m} w_j h_j(x) \qquad \text{[Equation 2]}$$

$$T = \{x_i, y_i\}_{i=1}^{p} \qquad \text{[Equation 3]}$$

y_i *is the* exit *f(x)* of the neuronal network plus an amount of noise.

Figure 4. The *n* components of the entry vector *x* and the activation base function h_j are lineally combined with the weight wj for the network exit *f(x)*.

The NNRBF is nonlinear, if the base functions are enabled for movement, change their size, or if there is more than one hidden layer. The NNRBF is linear when it is a single-layer and connects to a network with functions fixed in position as well as in size. Nonlinear optimization (Orr, 1996) is used only for regularization parameters in the ridge regression and in the optimal base function subgroup within the unidirectional selection.

The Mean Squared Error (MSE, Equation 1) is applied in the linear model of directed learning. Mean squares lead to the beginning of an optimization problem. Error is minimized applied equation 2 and 3.
If a weight (Figure 4) is adjusted to Equation 1, the error is added, as in the case of the ridge regression; then the regularization function Equation 4 is minimized plus the Equation 1.

$$C = \sum_{i=1}^{p} (y_i - f(x_i))^2 + \sum_{j=1}^{m} \lambda_j w_j^2, \qquad \text{[Equation 4]}$$

where λ_j is the regularization parameter; "j" is an index from 1 to m; m is the number of signals; and p is the signal window.

Wavelets

The Wavelets are function families of the type:

$$\psi_{a,b}(x) = \frac{1}{\sqrt{|a|}} \psi\left(\frac{x - b}{a}\right) \qquad \text{[Equation 5]}$$

where *a* equals expansion; *b* equals translation; and *x* equals sequence of signal points. The Wavelet is transformed from a signal and is represented by the following expression:

$$WT(f(x)) = f(x) * \psi = \frac{1}{a} \int f(t) \psi\left(\frac{x - t}{a}\right) dt \qquad \text{[Equation 6]}$$

Discreet analysis of a continued signal in time defines the parameters *a* and *b* with: $a = 2^j, b = k2^j, (j,k) \in Z^2$, and is named dyadic Wavelet. Later the Discreet Rapid Transformed Wavelet (DRTW) is used.

The transformed Wavelets are applied to the signal filters of high-pass filters, detail and low-pass filters, or approximation. The number of times the signal is filtered is determined by the decomposition level. To reduce the signal noise, the main idea eliminates components obtained in the transformed Wavelet that are under a certain threshold, or multiplies them by a certain pondering value before performing the inverse transformation. The most significant differences are found within the threshold or pondering value.

For noise reduction a nonlinear (proposed by Donoho, 1995) procedure is used called soft-thresholding, where only those coefficients of details under a certain threshold will be eliminated; the rest is pondered. The threshold calculation is obtained with statistical procedures (Novak et al, 2000) beginning with detail coefficients obtained by the transformed Wavelet. For natural noise reduction, it is necessary to consider a signal s(n):

$$s(n) = f(n) + \sigma e(n) \qquad \text{[Equation 7]}$$

where n is equally spaced, $f(n)$ represents noiseless signal, $e(n)$ is natural noise for our case, and σ means noise level.

The main noise reduction procedure is summarized in three fundamental steps:

1. Decomposition—a Wavelet is selected, an N level is chosen which will be the decomposition level, and the Wavelet decomposition calculations on an s signal are made on a N level.
2. Threshold Detail Coefficients (high pass)—for each level from 1 to N, a threshold is selected and applied to the soft-thresholding of detail coefficients.
3. Reconstruction—an inverse transformed Wavelet is calculated by using the original approximation coefficients of level N and a modified detail coefficients of level 1 to N.

The transformed Wavelet is used to obtain signal details at different levels by applying the threshold

$$C_{\sigma}(i,j) = \begin{cases} 0, si|C(i,j)\square| & \sigma = \sqrt{2\log(N)}\sigma \\ \text{por otro}, (C(i,j))(|C(i,j)| \square \square), si|C(i,j) \geq \square| \end{cases} \qquad \text{[Equation 8]}$$

To perform noise reduction in a nonlinear manner by employing soft-thresholding, the inverse transformed Wavelet is calculated to obtain the resulting signal. Ci,j represents coefficients of details obtained through the transformed Wavelet. The value of σ used for this threshold is given by the expression:

$$\sigma = media(|C(i,j)|)/0.6745 \qquad \text{[Equation 9]}$$

The final equation of the transformed Wavelet is defined by the sum of the last approximation and the sum of all the decompositions.

$$S = A_J + \sum_{j \square J} D_j \qquad \text{[Equation 10]}$$

Model Development

Data

In order to perform the initial tests, 36 seismic events were selected from the region of Cochabamba, Bolivia, for the year 2000 The coordinates of these events were –16° to –17° 5 latitude south and –64° to 67°.9 longitude west, and the events had magnitudes Ml greater than 3.0 (Table 2).

Model Scheme

The scheme in Figure 5 shows the information, procedure, and function flows used in the NNRBF first stage seismic localization model .

The initial stage is developed in the neural network environment, and introduces parameters for each of the 36 seismic events performed under directed training. Each event consists of up to 12,000 points (increased in some cases and reduced in others, as we should have uniform-sized samples.

To validate the NNRBF, test localization parameters for 35 seismic events were used as well as an independent event as an entry signal. Consequently the training matrix for this case is in the order of 12,000 x 35 (H, design matrix), and the event to be localized is outside the matrix. Once the test validation is concluded, more H matrix events may be incorporated, which increases the training group. The seismic events analyzed were registered in the national network (consisting of six stations), but in the first stage only data from the station closest to epicenters was used. This station also had a lower noise percentage.

NNFRB application

W weights (Figure 3) are adjusted so that the best solution between training signals and the entry signal ˆy may be found and a mean squared error (MSE) obtained. With the weight adjustment, a minimum or a maximum is obtained for each event (Table 2). These adjustments are selected by the MSE result obtained. For instance, event Nº8 (Table 2) renders a minimum of –0.1444 and a maximum of 0.1745, which are related to events Nº7 and 12, respectively, (Figure 6). The MSE value is lower for event Nº8 than it is for event Nº12, therefore provisional localization of event Nº8 is assumed for event Nº7. The process is performed for all 35 remaining events (Figure 6a).

Once all events were relocated (Geiger Method), the proposed model was evaluated. An optimal response of 13.9% was obtained, and a 77.8% regular result—a guide of the uncertainty in localization—plus a null result of 8.3% were obtained in relation to the 36th signal sample.

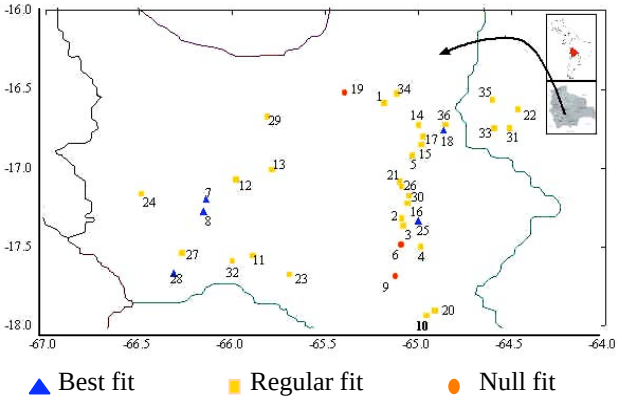

Map 1. Results obtained with NNFRB model.

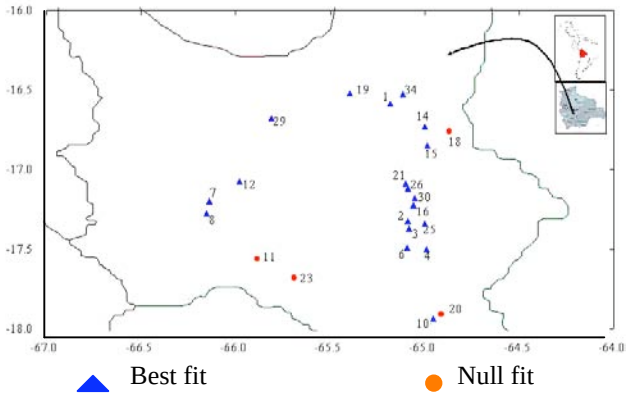

Map 2. Results with Neural Networks and Wavelet

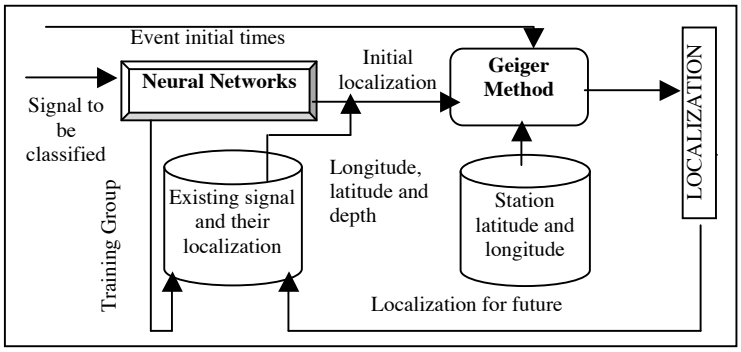

Figure 5. Schema of seismic localization model.

Table 2. Seismic events used in initial test the last column show the result obtained.

No.	Date	Time	Lat	Lon	Depth	MI	Best	Regular	Null	Result
1	16/01/00	10:55:11.775	-16.588	-65.183	65.00	3.32		MINIMUM		35
2	20/01/00	23:05:39.860	-17.323	-65.091	65.00	4.13		MINIMUM		21
3	21/01/00	03:35:16.869	-17.369	-65.083	65.00	4.19		MAXIMUM		16
4	21/01/00	05:34:56.200	-17.502	-64.990	16.06	3.14		MINIMUM		16
5	24/02/00	23:28:59.762	-16.921	-65.032	15.00	3.48		MAXIMUM		31
6	25/02/00	11:02:57.937	-17.489	-65.093	45.00	3.51			x	7
7	07/03/00	03:57:30.910	-17.197	-66.140	16.95	3.71	MINIMUM			8
8	07/03/00	03:59:36.234	-17.275	-66.154	40.00	3.57	MINIMUM			7
9	21/03/00	00:22:12.273	-17.687	-65.125	65.00	3.52			x	18
10	22/03/00	19:47:53.374	-17.907	-64.913	30.00	3.18		MAXIMUM		9
11	29/03/00	21:50:00.221	-17.559	-65.887	20.00	3.14		MAXIMUM		7
12	04/04/00	06:31:32.980	-17.076	-65.978	50.00	3.76		MAXIMUM		8
13	25/04/00	23:21:28.667	-17.013	-65.786	42.00	3.71		MAXIMUM		8
14	03/05/00	11:19:09.060	-16.730	-65.000	10.00	3.10		MINIMUM		34
15	03/05/00	15:44:17.249	-16.851	-64.985	31.00	3.28		MINIMUM		35
16	05/05/00	01:41:16.831	-17.224	-65.060	30.00	3.69		MINIMUM		9
17	07/05/00	07:43:58.882	-16.803	-64.978	8.00	4.16		MAXIMUM		34
18	24/05/00	09:16:37.859	-16.761	-64.869	10.00	3.75	MAXIMUM			36
19	03/06/00	15:36:49.793	-16.523	-65.397	25.00	3.20			x	4
20	14/07/00	01:06:52.358	-17.936	-64.956	30.00	3.61		MAXIMUM		9
21	28/07/00	18:57:09.935	-17.089	-65.102	15.00	3.56		MAXIMUM		16
22	29/07/00	13:30:02.771	-16.628	-64.468	10.00	3.13		MINIMUM		5
23	16/08/00	13:33:06.738	-17.680	-65.692	65.00	3.09		MAXIMUM		7
24	22/08/00	19:52:28.232	-17.165	-66.485	51.00	3.02		MINIMUM		27
25	25/08/00	19:43:32.564	-17.338	-65.001	40.00	3.08	MAXIMUM			2
26	08/09/00	05:23:24.860	-17.118	-65.090	15.00	3.06		MAXIMUM		9
27	15/09/00	19:38:23.284	-17.542	-66.267	21.00	3.81		MINIMUM		8
28	20/09/00	04:47:15.985	-17.669	-66.314	65.00	3.40	MAXIMUM			27
29	21/09/00	05:06:07.212	-16.676	-65.810	23.99	3.31		MINIMUM		12
30	27/09/00	03:06:03.683	-17.178	-65.052	35.00	3.26		MINIMUM		2
31	01/10/00	09:34:52.154	-16.750	-64.512	50.00	3.70		MINIMUM		21
32	03/10/00	15:00:43.571	-17.592	-65.997	65.00	3.35		MINIMUM		29
33	03/10/00	17:46:26.885	-16.750	-64.593	65.00	3.19		MAXIMUM		36
34	12/11/00	05:44:50.738	-16.529	-65.115	20.00	3.26		MINIMUM		18
35	30/11/00	15:44:54.595	-16.570	-64.604	65.00	3.83		MINIMUM		11
36	04/12/00	06:30:10.883	-16.724	-64.856	30.00	3.05		MINIMUM		31

We could not validate the localization obtained with the Geiger method and starting from results obtained with the NNRBF because the approximation between the entry signal and the training signals were inconsistent as a result of the signal variation in the first the coda phase.

Such an unexpected result drove us to seek the causes that render this NNRBF model inoperative. We performed a visual analysis of the coda signal and the type of phase, as well as measured the exactness of the first arrival reading (see Figure 7) and applied filters. Our results of this stage are conclusive and the main factor is each complex waveform that is affected by the crust structure under the central Andes and that, in some cases, leads to a wrong localization.

The visual analysis result indicated a signal association, which does not necessarily have the same localization but is in the same zone. For instance, as shown in Figure 8, this situation repeats itself throughout the analyzed region and allows a new analysis of 23 signals by introducing the Wavelet methodology.

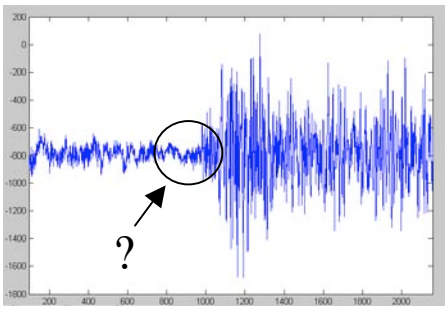

Figure 6. Unclear first arrival of event No 33, original signal

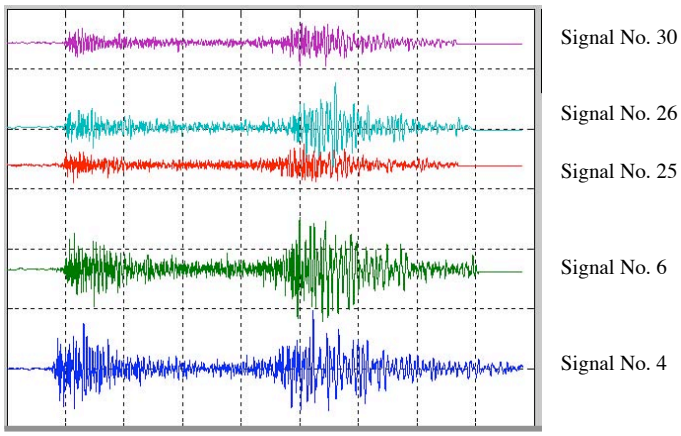

Figure 7. Similarities in five seismic events showing association among them as shown on Map 1.

Development with the Neural Networks and Wavelets

To optimize results, especially in the entry signals of the neural network, we introduce the Wavelet methodology and incorporate it in the localization model. We then proceed to transform the time domain entry signal without losing information. See Figure 9.

The process is performed with all 23 seismic events, Figure 6b that will be the database and entry to the neural network without considering the function of radial base. With the Wavelet method, we seek to obtain a representative model of each signal and we achieved this representation with the Haar family Wavelet.

In the Harr family ψ is the Wavelet; x is entry points and ϕ is the scale of wavelet function.

$$\begin{cases} \psi(x) = 1, & x \in [0, 0.5[\\ \psi(x) = -1, & x \in [0.5, 1[\\ \psi(x) = 0, & x \notin [0, 1[\\ \\ \phi(x) = 1, & x \in [0, 1] \\ \phi(x) = 0, & x \notin [0, 1] \end{cases}$$

The Wden (MatLab) tool is applied in the Wavelet equations in order to reduce noise. Syntax of this function follows:

xd = wden(x,'sqtwolog','min',5,'Haar');

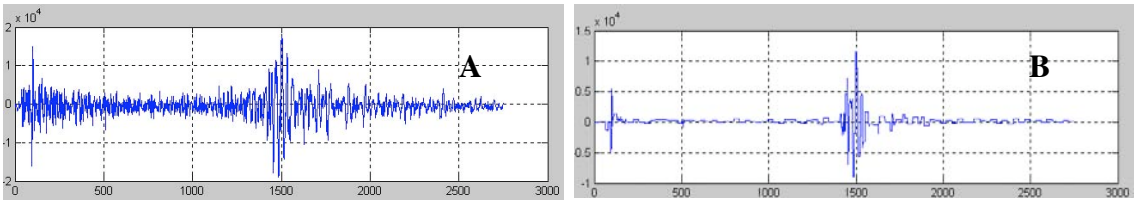

Figure 9. Signal no. 15, A) original signal B) transformed signal

where x is the entry signal to transform with the defined function 'sqtwolog' as the parameter that calculates each of the detail coefficients (high pass)' threshold; 's' is soft - thresholding (a noise reduction process); 'min' is the

parameter that does not refer to Gaussian noise and is used in the decomposition level that depends on the noise level; the '5' function value relates to the decomposition level,; and "Haar" refers to the Wavelet Haar family. The transformed signal is defined as xd, which is the entry parameter of the neuronal network.

The results featured in Table 3 reflect the scale conversion process of the entry signal. Later the Wavelet transformation is performed and finally the signal is classified in the neural network, finding a MSE for each of the events. These steps are performed for each one of the iterations (1^{st}, 2^{nd}, 3^{rd}, 4^{th}) independently.

Table 3. Results applying Wavelets and neural networks to 23 earthquakes

Nº	1 st	2 nd	3 rd	4 th	MSE	Result
1	19	18	25	6	8.207 EXP(-6)	1
2	21	3	21	21	11.545 EXP(-4)	1
3	2	2	26	2	11.444 EXP(-4)	1
4	21	12	30	21	9.936 EXP(-6)	1
6	21	7	25	1	10.350 EXP(-6)	1
7	8	8	8	8	14.187 EXP(-5)	1
8	7	7	7	7	7.658 EXP(-5)	1
10	4	7	30	20	4.197 EXP(-6)	1
11	20	18	30	30	2.650 EXP(-6)	0
12	8	7	29	8	19.297 EXP(-5)	1
14	15	18	15	15	26.475 EXP(-7)	1
15	14	18	14	14	24.991 EXP(-7)	1
16	18	21	26	6	40.788 EXP(-5)	1
18	1	23	30	30	56.556 EXP(-6)	0
19	1	18	30	25	10.082 EXP(-6)	1
20	18	18	30	30	5.730 EXP(-6)	0
21	18	16	4	4	16.598 EXP(-5)	1
23	1	18	30	30	6.655 EXP(-6)	0
25	1	18	30	26	20.594 EXP(-7)	1
26	1	7	25	25	46.925 EXP(-7)	1
29	12	12	30	11	19.463 EXP(-6)	1
30	18	8	25	15	18.040 EXP(-7)	1
34	18	23	30	1	30.501 EXP(-6)	1

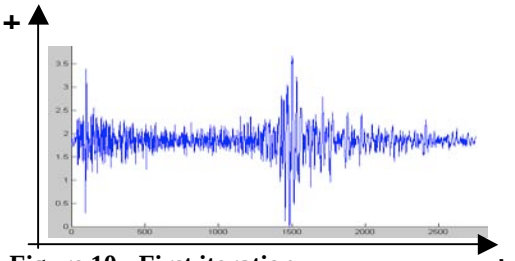

Figure 10. -First iteration

In the first iteration (Figure 10), the scale is changed and seismic amplitudes are converted to positive values. This result is obtained by finding the highest negative values, inverting their sign, and adding them to each of the signal points. Next the Wavelet transformation is performed and finally the result are obtained after the signal is classified with the neural network

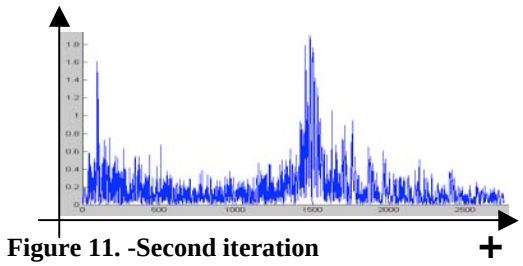

Figure 11. -Second iteration

In the 2^{nd} iteration (Figure 11), some amplitudes of the seismic event are converted into a positive. The negative values of the signal are inverted. Next the Wavelet transformation is performed, and finally the results are obtained after the signal is classified with the neural network

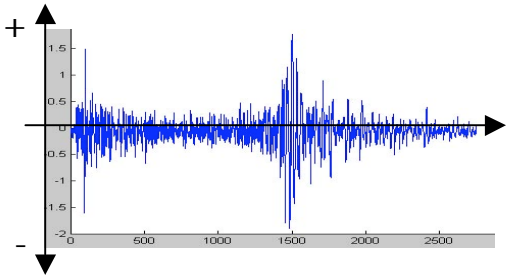

Figure 12. -Third iteration

In the 3rd iteration (Figure 12), the scale is changed in the positive and negative values; but the first value of the seismic event's amplitude begins at ZERO. The same values is added or subtracted from the first. Next the Wavelet transformation is performed, and finally the result are obtained after the signal is classified with the neural network

In the 4th iteration the same scale changes are performed as in the 1st iteration, with the sole difference being that when Wavelets are applied, decomposition is not a level 5 (as in the case of previous iterations), but a level 1. Next the Wavelet transformation is performed and finally the results are obtained after the signal is classified with the neural network

The first four columns in Table 3 indicate the identification of the event to be localized. These columns are responses to each of the iterations related to identification of the event associated with the entry signal. For instance, event Nº8 is similar to the 1st iteration of Nº15. We note that the remaining iterations provide us with the same event number, thus ensuring a very dependable localization. By contrast, the opposite happened with event Nº34 because of the fact that its optimal localization is found in the 4th iteration. We also note that results for event N 34 are different in the previous iterations. Optimal result choice is based on the MSE calculated by the neural network. The example has a MSE of 30.501 10^{-6}, which is lower if related to the other iterations' results.

The number "1" in the last column of Table 3 means an optimal result is related with the previous localization. A total of 83% functionality and 17% of bad previous localization was obtained from the entire study sample as a result of the association of events that were more localized in their epicenters.

CONCLUSIONS AND RECOMMENDATIONS

A first model (or method) for automatic localization, based on a Neuronal Networks on Radial Bases Functions (NNRBF) could not be validated as the approximation between the entry signal and the training signals are inconsistent resulting from the signal variation in the first stage coda. The first test was performed with 36 seismic events taken from the year 2000 and located in the region of Cochabamba - Bolivia (magnitudes greater than 3), and the results were an optimal response of 13.9%, a 77.8% regular result, and a null result of 8.3%

After a visual analysis of the coda signal characteristic in each event, a second model proposed based on neural networks and wavelets using three main steps: Decomposition; Threshold Detail Coefficients, and Reconstruction. These steps are performed by four independent iterations. Results reflected 83% functionality and 17% show a bad response.

We recommend continuing to improve the Wavelet model proposed by introducing other traditional location methodsand applying other Wavelets families. It will be necessary to use the wavelet methodology in order to identify the phases in the p code; this information will be introduced in the final model. Once the model is validated, we will apply it in other regions of Bolivia and other sites.

REFERENCES

Aliaga, H. P. (2002), Modelo de Localización Sísmica con Parámetros Sismológicos Aplicando la Red Neuronal con Funciones de Base Radial y la Metodología de Geiger, *Tesis Universidad Católica Boliviana*, La Paz –Bolivia.

Avila, G. (2000), Métodos de Localización Aplicados a Sismos Ocurridos en Bolivia, *Tesis universidad Técnica de Oruro*, Oruro- Bolivia.

Bitmead, R. (1993), Introducción a las Redes Neuronales, *Grupo de Tratamiento Avanzado de Señales, Universidad de Cantabria*.

Donoho, D. L. (1995), De-noising by Soft-thresholding, *IEEE Trans. Information Theory,* vol. 41, num. 3, pp.612-617.

Hilera, J. R. y V. J. Martínez (1995), Redes Neuronales Artificiales.

Kohonen, T. (1984), Neuro Computación, *Escuela Técnica Superior de Ingenieria Informatica, Universidad de Granada*, España.

Kung, S. Y. (1993), Digital Neural Networks.

Misiti M. y et al (1997-2000), Wavelet Toolbox for Use with MatLab, *The MathWorks Inc.,* ver 2.

Novák, D. y et al (2000), Denoising Electrocardiogram Signal Using Adaptive Wavelets, *Proceeding of the 15th Biennial Eurasip Conference BIOSIGNAL,* pp 18-20.

Orr, M. J. L. (1996), Introducción a las Redes con Funciones de Base Radial, *Universidad de Edimburgo*, Escocia.

Pressman, R. S. (1993), Ingeniería de Software, 3ra. Ed.

Rumbaug, M. y et al (1996), Modelado y Diseño Orientado Objetos OMT, España.

Wallace, T. C. (1996), Modern Global Seismology, pp 217-231.